A nanoscale resolution assay of flow-induced platelet microaggregation

Mikroagregacja płytek indukowana przepływem – badanie w nanorozdzielczości

M.J. Santos-Martínez[1], C. Medina[1], A. Prina-Mello[2], J. Conroy[3], S.P. Samuels[3], Y. Volkov[2,3], M.W. Radomski[1,2]

[1]School of Pharmacy and Pharmaceutical Sciences, Panoz Institute, Trinity College Dublin, Dublin 2, Ireland
[2]Centre for Research on Adaptive Nanostructures and Nanodevices, Trinity College Dublin, Dublin 2, Ireland
[3]Department of Clinical Medicine, Institute of Molecular Medicine Trinity College Dublin, Dublin 8, Ireland

Kardiochirurgia i Torakochirurgia Polska 2010; 7 (4): 365–375

Abstract

Background: Platelet aggregation is essential for vascular haemostasis and thrombosis. Inhibition of platelet aggregation underpins the pharmacological and clinical effects of antiplatelet drugs. These effects are commonly quantified using methods that assess platelet aggregation under no-flow conditions in macroscale. These devices neither mimic the conditions found in human microvasculature nor detect microaggregates.

Aim: The aim of our study was to develop a new method of flow-induced platelet microaggregation using a commercially available (Q-Sense^{TM} E_4 system) nanoscale resolution device, Quartz Crystal Microbalance with Dissipation (QCM-D), that measures mass deposition on sensor crystals as changes in their frequency of vibrations *f* and energy dissipation *D*.

Material and methods: Human platelets were perfused through QCM-D and *f* and *D* were recorded in real time. Phase-contrast, confocal imaging, atomic force microscopy and flow cytometry were also used to study flow-induced platelet microaggregate formation on the surface of fibrinogen-coated crystals.

Results: Microaggregates were detected by the device by changes in *f* and *D* in a platelet concentration-, flow- and shear stress-dependent manner, confined to the sensor surface and imaged by phase-contrast, confocal and atomic force microscopy.

Conclusions: QCM-D is a sensitive device capable of measuring flow-induced platelet microaggregation.

Key words: atomic force microscopy, microaggregation, platelets, quartz crystal microbalance.

Streszczenie

Wstęp: Agregacja płytek jest niezbędna w hemostazie naczyniowej i zakrzepicy. Hamowanie agregacji płytek wzmacnia farmakologiczne i kliniczne efekty leków przeciwpłytkowych. Efekty te są powszechnie mierzone z użyciem metod szacujących agregację płytek w warunkach bezprzepływowych (*no flow conditions*) w makroskali. Urządzenia te nie imitują warunków panujących w ludzkim układzie mikronaczyniowym ani też nie wykrywają mikroagregatów.

Cel pracy: Celem pracy było stworzenie nowej metody mikroagregacji płytek indukowanej przepływem z użyciem dostępnego na rynku (Q-Sense^{TM} E_4 system) urządzenia o nanorozdzielczości (*nanoscale resolution device*) Quartz Crystal Microbalance with Dissipation (QCM-D) mierzącego składowanie mas na kryształach czujnika jako zmiany w częstotliwości wibracji *f* oraz rozproszeniu energii *D*.

Materiał i metody: Ludzkie płytki poddano perfuzji z zastosowaniem QCM-D; *f* i *D* były rejestrowane w czasie rzeczywistym. Zastosowano również mikroskopię z kontrastem fazowym, obrazowanie konfokalne, mikroskopię sił atomowych oraz cytometrię przepływową w celu zbadania mikroagregatów pytek indukowanych przepływem tworzących się na powierzchni kryształów pokrytych fibrynogenem.

Wyniki: Urządzenie wykryło mikroagregaty poprzez zmiany w *f* i *D* w sposób zależny od stężenia płytek, przepływu oraz sił ścinających; ograniczone do powierzchni czujnika i obrazowane mikroskopią z kontrastem fazowym, konfokalną oraz sił atomowych.

Wnioski: Quartz Crystal Microbalance with Dissipation jest urządzeniem o dużej czułości umożliwiającym pomiar mikroagregatów płytek indukowanych przepływem.

Słowa kluczowe: mikroskopia sił atomowych, mikroagregacja, płytki, mikrowaga kwarcowa.

Adres do korespondencji: Prof. Marek Radomski, School of Pharmacy and Pharmaceutical Sciences, Panoz Institute, Trinity College Dublin, Dublin 2, Ireland, Tel. 353-1-8962819, Fax 353-1-8963367, Email: marek.radomski@tcd.ie

Background

Platelets are blood elements that play a crucial role in vascular haemostasis. In response to vascular damage, platelets interact with subendothelial proteins, resulting in a haemostatic plug. Plasma and subendothelium proteins including fibrinogen, collagen, and von Willebrand factor (vWF) mediate platelet adhesion and aggregation by engaging with platelet receptor proteins. GPIb, the vWF binding subunit of the GPIb/V/IX receptor, mediates mainly platelet adhesion to the endothelium [1, 2]. Platelets then change shape through reorganization of the cytoskeleton, leading to the generation of mediators such as thromboxane A_2 (TXA_2) [3], adenosine diphosphate (ADP) [4] and matrix metalloproteinase-2 (MMP-2) [5] that recruit more platelets to the aggregate. The GPIIb/IIIa receptor is essential for this process, since it allows fibrinogen binding to the receptors of adjacent platelets [6].

Over the past 50 years various methods have been used to study platelet aggregation. O'Brien first reported the use of a strong hand lens with powerful cross illumination to monitor platelet aggregation [7]. Later, Born developed a simple spectrophotometer device (light aggregometer) that recorded changes in light transmission in response to aggregation induced by agonists in stirred platelets [8].

The method had a profound effect on platelet aggregation research and similar devices based on measurement of light scattering or electrical impedance [9] are routinely used worldwide. However, these instruments do not detect the initial aggregation process which is characterized by the formation of microaggregates. Platelet function measurements using vessel wall damage- and flow-mimicking devices such as cone and plate analyser, platelet function analyser 100, coaxial cylinder couette or annular and parallel perfusion chambers have limited sensitivity and specificity and do not correlate well with the light aggregometer, which still remains the "gold standard" of platelet function testing [10-15].

In order to overcome these problems we have used a Quartz Crystal Microbalance with Dissipation (QCM-D). The principle of analysis of QCM is based on the resonance frequency *f* of a quartz crystal induced by applying an alternating electric field across the crystal. An increase in mass bound to the quartz surface causes the crystal's oscillation frequency *f* to decrease (negative *f* shift) and it has been shown that for rigid, evenly distributed, and sufficiently thin adsorbed layers *f* is proportional to the mass. In this way, the QCM operates as a very sensitive balance and the mass can be calculated with nanogram sensitivity [16]. Changes in *f* as a result of platelet adhesion on quartz crystals have been reported previously by Matsuda [17] and Kawakami [18] using a custom-made QCM. However, when a soft or thick layer is bound to the crystal there is a high dissipation *D* shift and the damping or *D* of the crystal's oscillation reveals the film's softness (viscoelasticity). In this particular case the mass can be underestimated by measuring only *f*. Therefore, the combined information from changes in *f* and *D* is superior to *f* measurements alone [19, 20]. Using a QCM-D both parameters can be monitored simultaneously in real time and the formation of thin films (nm) of biological materials such as proteins or cells can be characterized by measuring both *f* and *D* [21, 22].

We used a commercially available QCM-D to design a novel method to measure in real time platelet microaggregation under low flow conditions.

Materials and methods

Reagents

All reagents were purchased from Sigma-Aldrich (Dublin, Ireland) unless otherwise indicated.

Blood collection and platelet isolation

Blood was collected from healthy volunteers who had not taken any drugs known to affect platelet function for at least 14 days prior to the study. Platelet-rich plasma (PRP) was prepared from blood as previously described [23] and diluted with PBS at final concentrations from 50,000 to 210,000 platelets μL^{-1}. Platelet-poor plasma (PPP) was used as a control for protein plasma deposition.

Quartz Crystal Microbalance with Dissipation

The QCM-D from Q-Sense (Q-Sense^{TM} E_4 system, Q-Sense AB, Sweden) has four temperature and flow-controlled modules set up in parallel configuration. The heart of the system is a quartz crystal sensor that is placed in a chamber inside the module. Samples are perfused using a peristaltic microflow system (ISMATEC, IMS 935).

For the study of platelet aggregation, polystyrene-coated (PC) quartz crystals were used as sensors following coating with fibrinogen. Fibrinogen-uncoated PC-quartz crystals were used as controls. For fibrinogen coating sensors were placed in fibrinogen dissolved in phosphate buffered saline (PBS) (100 $\mu g\ mL^{-1}$) for one hour at room temperature. Sensors were mounted on the flow chamber and PRP (50,000; 100,000; 150,000 and 210,000 platelets μL^{-1}) was perfused through the device at 37°C and platelet aggregation was monitored in real time by the acquisition Q-Sense software ($QSoft_{401}$) and measured as *f* and *D*.

To study the effects of increasing concentrations of platelets, PPP and PRP (100,000; 150,000 and 210,000 platelets μL^{-1}) were perfused at 50 and 100 $\mu L\ min^{-1}$ for up to 60 minutes and the concentration-response curves were generated.

To analyse the effects of flow rates and platelet concentrations on shear stress, PRP (210,000 platelets μL^{-1}) was perfused through the system at a fixed flow rate (10, 20, 50 and 100 $\mu L\ min^{-1}$) for 30 minutes and platelet aggregation was monitored and measured as changes in *f* and *D*.

Phase-contrast microscopy

The formation of platelet aggregates on the crystal surface was studied using a Zeiss microscope (Axiovert 200M, UK). First, PPP and PRP suspensions were perfused on

fibrinogen-coated PC-quartz crystals for 30 minutes through the device. The crystals were then taken for phase-contrast microscopy using a 20x objective. Photomicrographs were captured using a digital camera and Zeiss software (Axiovision 4.7).

Confocal microscopy

For the study of activated platelets PRP was perfused on fibrinogen-coated PC-quartz crystals for 30 minutes. Afterwards, crystals were placed in a 24-well plate and washed three times with PBS. Each sample was then treated with fluorescein isothiocyanate (FITC) conjugated PAC-1 (BD Biosciences, UK/Ireland) (150 µL) for 30 minutes in the dark. Platelets were then fixed with 2% formaldehyde for 30 minutes at room temperature and permeabilized with 0.1% triton for 3 minutes. Finally, samples were stained with phalloidin actin (Invitrogen, USA) (1 : 200 dilution) for 1 hour at room temperature, and mounted on a glass slide with mounting medium. For the study of resting platelets, platelets were treated in suspension and mounted on a glass slide. In both cases confocal images were taken using a 63x oil immersion objective, with a numerical aperture of 1.4, on a Zeiss LSM 510 Meta system (UK). The samples were excited using 488 nm and 561 nm and emission filters of band-pass 505-550 nm and long-pass 575 nm, respectively.

Atomic force microscopy

For the atomic force microscopy (AFM) imaging PRP was perfused on fibrinogen-coated PC-quartz crystals for 30 minutes.

Afterwards, samples were fixed using 2.5% glutaraldehyde for 30 minutes at 37°C. Platelets were then dehydrated through ascending grades of ethanol (60% for 20 minutes, 80% for 20 minutes, 90% for 20 minutes and finally 100% for 30 minutes repeated once). Thereafter, crystals were mounted onto microscope slides facing upwards. The crystal-on-slide was mounted onto the microscope and clipped down to ensure no movement during acquisition. Images were then taken using an Ntegra Spectra (NT-MDT, Russia) AFM/Raman system. Imaging was carried out in dry-phase, semi-contact AFM with a silicon-nitride tip (NSG10, Golden silicon probes). The resonance frequency of the tip was found to be 280 KHz. Height AFM images, 70 µm x 70 µm scans, were taken five times for each sample, around the central area of the crystal, at 0.55 Hz. Image analysis was carried out on the height images using the Nova software (filter Fit Lines-X was used followed by subtract plane and finally grain analysis).

Flow cytometry

In order to analyse receptor expression on the surface of individual platelets and to minimize platelet activation caused by sample preparation procedures, no stirring or vortexing steps were used. The abundance of P-selectin on the surface of platelets after perfusion of PRP through the system, in the presence or absence of thrombin receptor-activating peptide (TRAP 25 µmol L^{-1}) was measured by flow cytometry as previously described [24]. Resting platelets were used as a control. After collection samples were incubated in the dark for 5 minutes at room temperature in the presence of saturating concentrations (10 µg mL^{-1}) of P-selectin (CD62P-APC from BD Biosciences, UK/Ireland). Following incubation, samples were diluted in FACS Flow fluid and analysed within 5 minutes using a BD FACSArray (BD Biosciences, Oxford, UK). The instrument was set up to measure the size (forward scatter), granularity (side scatter) and cell fluorescence. A two-dimensional analysis gate of forward and side scatter was drawn in order to include single platelets and exclude platelet aggregates and microparticles. Antibody binding was measured by analysing individual platelets for fluorescence.

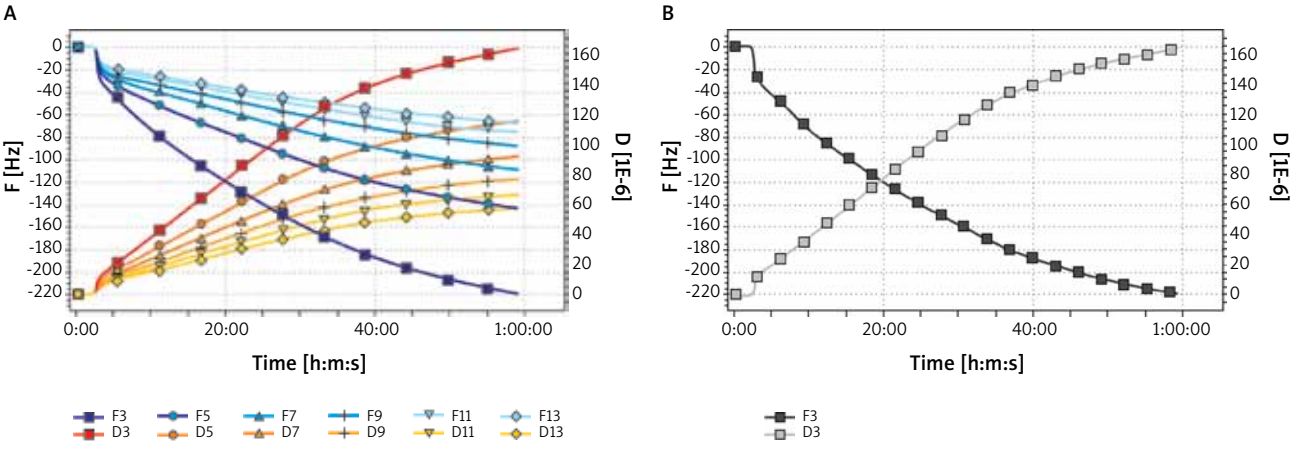

Fig. 1A–B. Effects of physiological concentration of platelets on frequency *f* and energy dissipation *D*. Perfusion of polystyrene-coated quartz crystals with PRP (210,000 platelets/µL) led to a decrease in *f* and increase in *D*. A. Blue lines correspond to changes in *f* and red-orange lines correspond to changes in *D* for six different overtones (3rd, 5th, 7th, 9th, 11th and 13th) measured during the experiment. The actual values for *f* are shown in the left axis and for *D* in the right axis vs time. B. Data from the experiment shown in A. related to the 3rd overtone

The mean fluorescence intensity was determined after correction for cell autofluorescence. For each sample, the fluorescence was analysed using a logarithmic scale. Fluorescence histograms were obtained for 10,000 individual events. Data were analysed using BD FACSArray system software 1.0.3.

Rheology

The platelet aggregation rheology study was carried out based on the dimensions of the module chamber and assuming laminar flow along the crystal active measurement area. The volume ric flow rate Q injected through the peristaltic pumping system was considered incrementally fixed at 10, 20,50 and 100 µL min^{-1}. Shear rates and shear stresses on different platelet concentrations were calculated based on the PRP rheological changes at the same conditions where the experiments were performed, at 37°C. The mean velocity within the chamber during each experiment was calculated as $v_{mean} = Q/(w \cdot h)$, where Q is the flow rate, w is the width and h the height of the chamber inside the module.

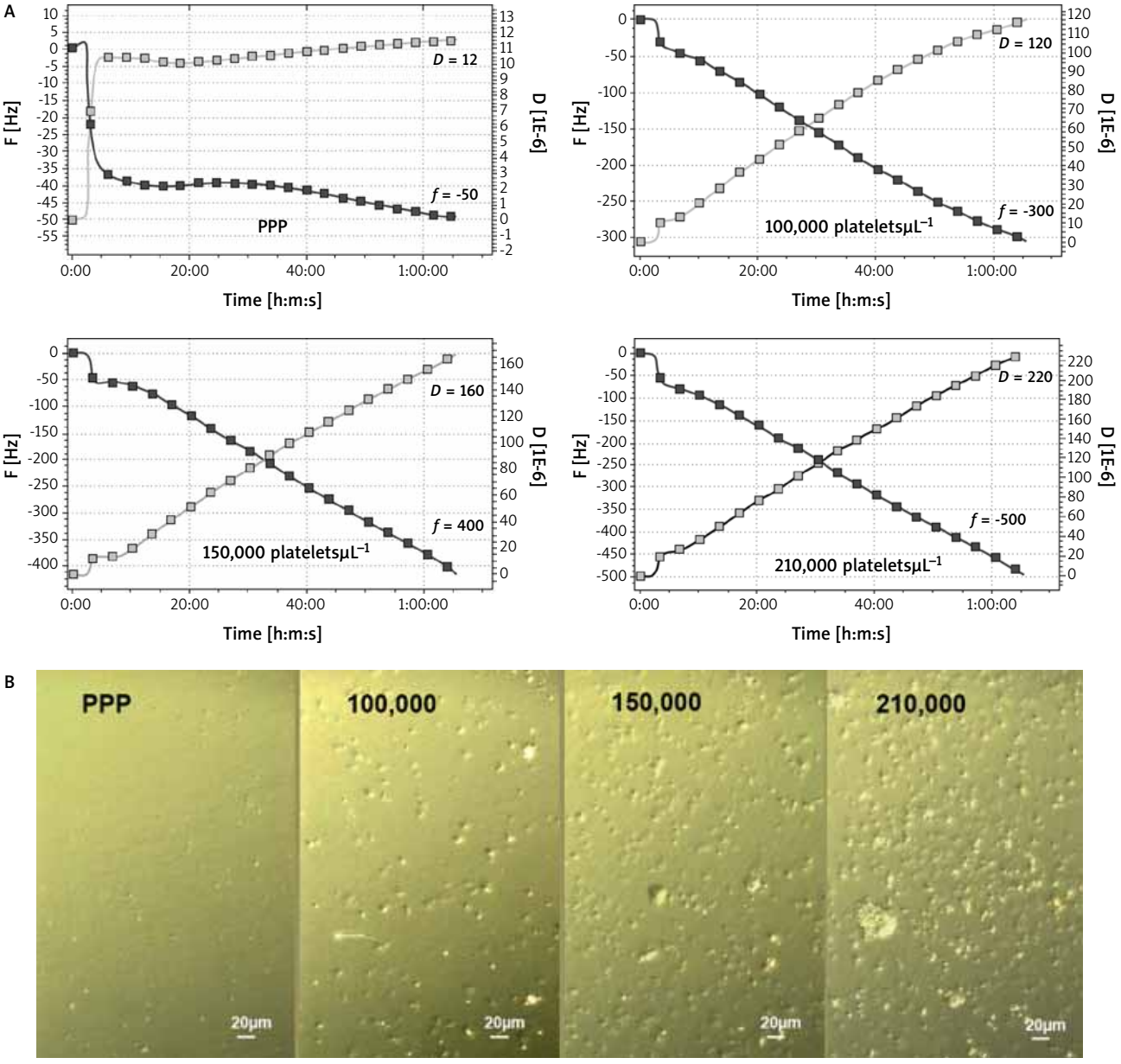

Fig. 2A–B. Effects of platelet concentrations on frequency *f*, energy dissipation *D* and platelet deposition on crystals. Perfusion of fibrinogen-coated PC-quartz crystals with PRP leads to platelet aggregation. A. Representative tracings from the 3rd overtone recorded by the device show the effects of platelet-poor plasma (PPP) and increasing concentrations of platelets: 100,000; 150,000 and 210,000 platelets/µL on *f* (dark squares) and *D* (light squares). The perfusion of fibrinogen-coated PC-quartz crystals led to a concentration-dependent decrease in *f* and increase in *D*. B. Representative micrographs of the surface of fibrinogen-coated PC-quartz crystals as viewed by phase-contrast microscopy show increased accumulation of platelet aggregates following perfusion with PRP (100,000; 150,000 and 210,000 platelets/µL) but not with PPP

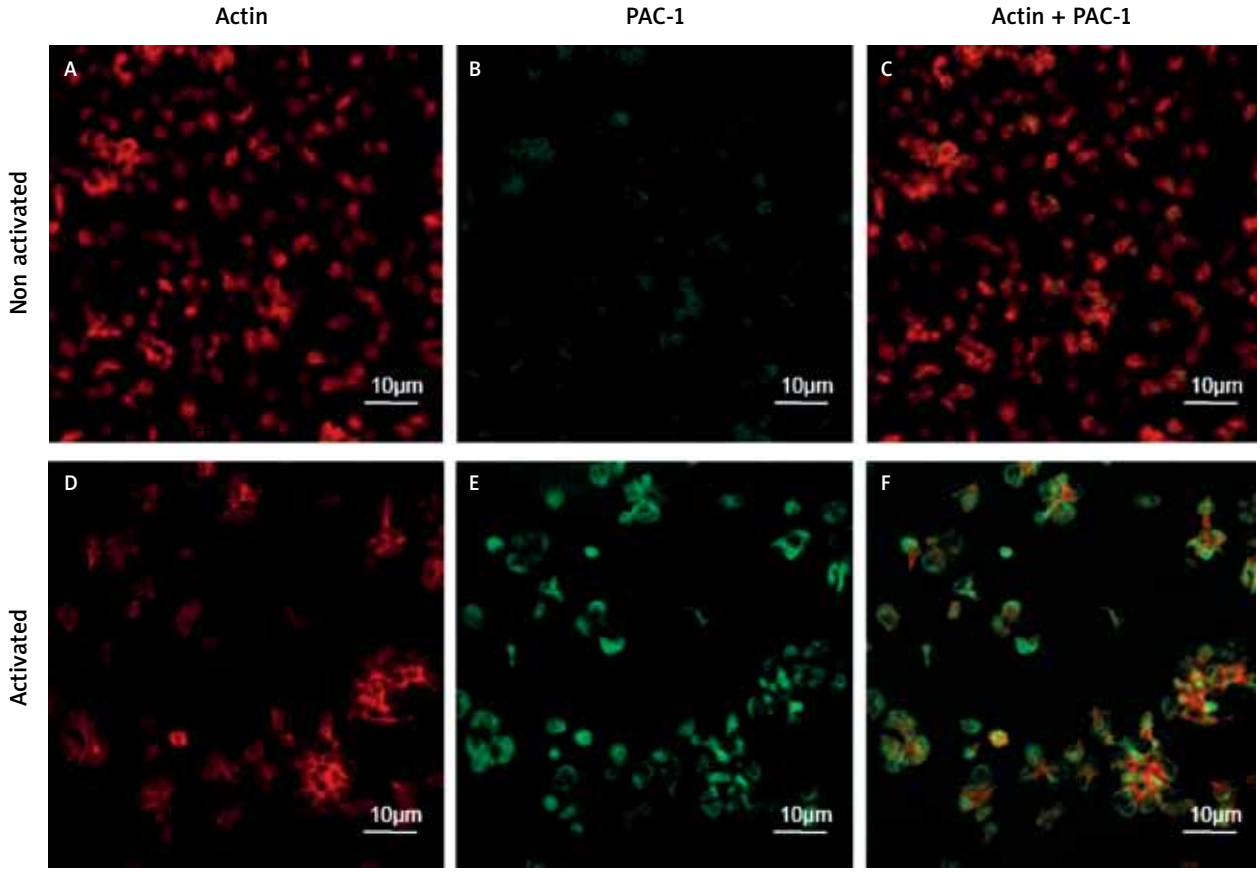

Fig. 3A–F. Co-localization of activated GPIIb/IIIa (PAC-1) with actin in platelet cytoskeleton upon aggregation on sensor crystals. Confocal microscopy of resting (A–C) and activated (D–F) platelets depict the interactions between PAC-1, actin and cytoskeleton. Staining was performed with fluorescent-labelled antibodies against actin (A and D) or activated GPIIb/IIIa (PAC-1) (B and E). Digital merging of actin and PAC-1 images (C and F) shows co-localization of actin- and PAC-1-labelled structures

The shear rate γ in the middle of the crystal sensing area was calculated by $\gamma = \delta\, v_{mean}/h$, where density δ was calculated based on the mass for the volume used. The shear stress τ was given by the formula $\tau = \delta \cdot v_{mean}\, \eta/h$, where η is the dynamic viscosity. The dynamic viscosity of PRP preparations (at final concentrations of 100,000; 150,000 and 210,000 platelets μL^{-1}) was measured using a vibro-viscosimeter (SV-10 sine wave SV-10, A&D, USA). Prostacyclin (100 ng mL^{-1}) was added to each sample prior to measurement to inhibit platelet aggregation during the acquisition.

Q-Tools analysis using Voigt-based viscoelastic model

Assuming the deposition of a homogeneous layer across the crystal, it is possible, using the analysing Q-Tools software (Q-Sense AB, Sweden), to perform modelling of the raw data from the Q-Sense software ($QSoft_{401}$) and calculate the layer thickness and accumulation of mass. Changes in *f* and *D* induced by deposition of platelets and plasma proteins were measured simultaneously at the 3rd, 5th and 7th overtones and modelled to calculate the thickness of the layer and estimate the mass deposited on the crystal surface.

Statistics

Results are expressed as *f* and *D* (from the 3rd overtone) or as percentage of aggregation (where the values for 210,000 platelets μL^{-1} on fibrinogen-coated PC-quartz crystals were considered as 100% of aggregation) of at least three independent experiments. All means are reported with standard deviation. Data were analysed using GraphPad Prism 5 software. One-way analyses of variance, repeated measures ANOVA and Dunnett's or Tukey-Kramer's multiple comparisons post test were performed, where appropriate. Statistical significance was considered when $P < 0.05$.

Results

Perfusion of sensor crystals with platelets leads to aggregation

The perfusion of physiological concentrations of platelets (210,000 platelets μL^{-1}) on PC-quartz crystals induced a decrease in *f* and an increase in *D*, indicating the deposition of platelets on the sensor surface (Fig. 1).

The effects of different concentrations of platelets perfused on fibrinogen-coated and fibrinogen-uncoated PC-quartz crystals at a flow rate of 50 and 100 µL min^{-1} were investigated. Platelet-poor plasma and increased

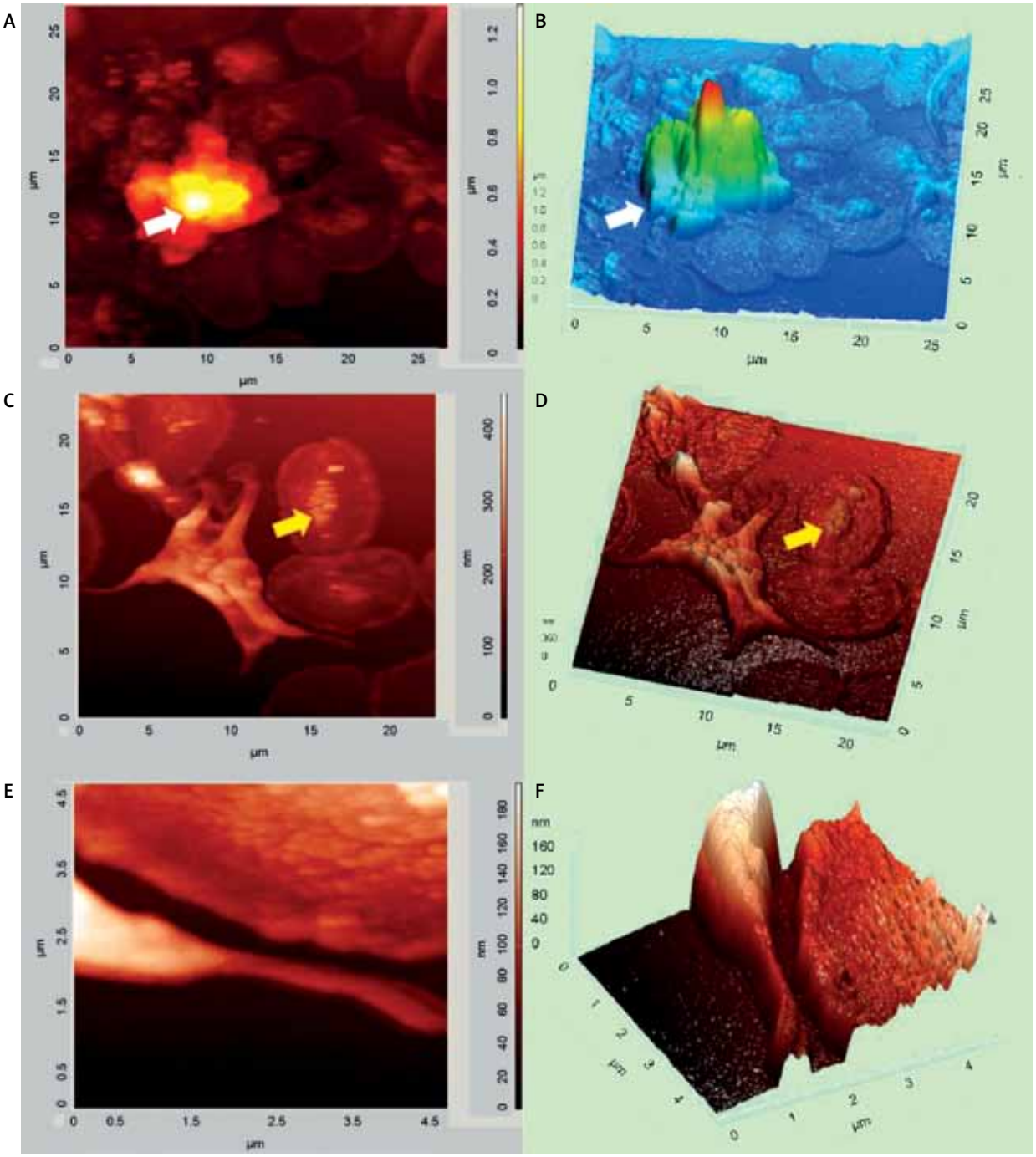

Fig. 4A–F. Activated single platelets as imaged by atomic force microscopy (AFM). Representative AFM height-based images with AFM-3D topography of platelets. Panels A and B show images of platelet aggregates (white arrows). Panels C, D, E and F reveal the sequence of early and later stages of aggregate formation including spreading and shape change. Granular centralization and budding contributes to the formation of a pseudonucleus (fried egg-like) structure (yellow arrows) in single platelets (C and D) and the appearance of finger-like projections (pseudopodia) heralds the later stages of platelet activation (E and F)

concentrations of platelets were perfused across the sensors for up to 60 minutes. Perfusion of PRP across fibrinogen-coated sensors led to a concentration-dependent decrease in *f* and increase in *D* when compared to PPP (Fig. 2A). These effects were confirmed by phase-contrast microscopy that showed the presence of platelet aggregates on the surface of crystals (Fig. 2B). Furthermore, a cytoskeleton reorganisation, activation of GPIIb/IIIa and the formation of pseudonucleus and pseudopodia were detected by confocal and AFM (Fig. 3 and Fig. 4). The perfusion of fibrinogen-uncoated PC-quartz crystals also led to platelet aggregation. However, these effects were lower when compared to fibrinogen-coated PC-quartz crystals. When traces recorded for fibrinogen-uncoated and fibrinogen-

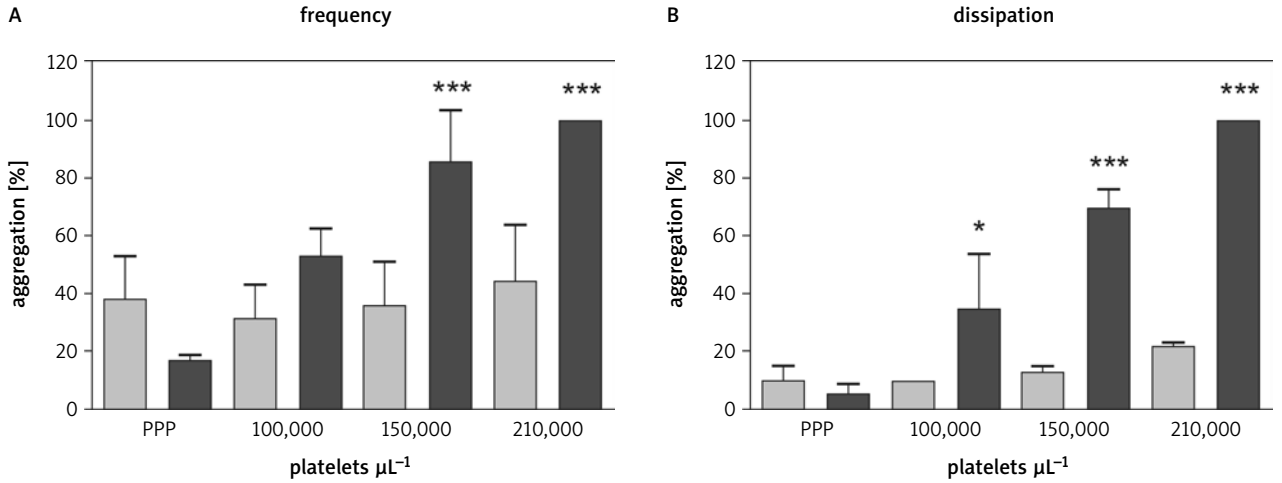

Fig. 5. Effects of platelet-poor plasma and increasing concentrations of platelets perfused on fibrinogen-uncoated and fibrinogen-coated PC-quartz crystals at 100 µL/min for 30 minutes. Blue bars correspond to the values for *f* after the perfusion of platelet-poor plasma (PPP) and different concentrations of PRP on fibrinogen-uncoated PC-quartz crystals (light blue) and fibrinogen-coated PC-quartz crystals (dark blue). The values for *D* are represented by yellow bars (fibrinogen-uncoated PC-quartz crystals) and red bars (fibrinogen-coated PC-quartz crystals). Data are expressed as mean ± SD. *P < 0.05 coated vs uncoated, ***P < 0.001 coated vs uncoated

coated PC-quartz crystals were analysed and compared at 50 and 100 µL min^{-1} and after 15, 30, 45 and 60 minutes of perfusion of PRP, significant differences were found after perfusion of physiological concentrations of platelets at 100 µL min^{-1} for 30 minutes (repeated measures ANOVA, $n = 3$, P_f and $P_D < 0.0001$, Tukey's Multiple Comparison Test, $P < 0.05$ coated vs uncoated) (Fig. 5). Perfusion of fibrinogen-coated PC-quartz crystals with PRP at 50,000 platelets μL^{-1} also led to a decrease in *f* and increase in *D* (Fig. 6).

Platelets not associated with the sensor surface were not activated, as shown by low abundance of P-selectin on the platelet surface in perfusate measured by flow cytometry. However, these platelets could be activated in the presence of soluble agonists such as TRAP (repeated measures of ANOVA, $n = 3$, $P < 0.001$ vs control) (Fig. 7).

Rheology

The influence of flow rates and platelet concentrations on platelet aggregation and shear stress inside the perfusion chamber within the crystal active measurement area was also studied. The perfusion of PRP (210,000 platelets μL^{-1}) at 10, 20, 50 and 100 µL min^{-1} resulted in a significant decrease in *f* and increase in *D* with maximal effect at 50 and 100 µL min^{-1} (One-way ANOVA; $n = 3$; $P_f = 0.0003$; $P_D = 0.0008$; Tukey's Multiple Comparison Test, $P < 0.01$ vs 10 µL min^{-1}). The effect of bulk shear stress on platelet aggregation was calculated for incremental flow rates (10, 20, 50 and 100 µL min^{-1}) and increased concentrations of platelets (100,000; 150,000 and 210,000 platelets μL^{-1}) at 37°C, ranging between 0.2 and 4.0 dyne cm^{-2} (Fig. 8, Table I).

Q-Tools analysis using Voigt-based viscoelastic model

Considerable differences in the fitting depending on the donor and the experimental conditions were found using the Q-Tools software. AFM imaging was performed on samples where the modelling was applied and the image analysis on the height images was carried out to evaluate the accuracy of the Q-Tools modelling. The average heights for the platelet aggregates calculated by AFM and the ones obtained using the Voigt-based model by the Q-Tools software are shown in Table II.

Discussion

The main objective of our work was to characterize low flow-induced platelet microaggregation using a nanoscale resolution device, QCM-D. We used PRP for these experiments as the use of whole blood would necessitate constant mixing of platelet samples to be perfused over a long period of time (up to 60 minutes) and this could result in platelet activation.

Since nanoscale devices have great sensitivity and measure deposition of mass in nanograms, the first question was whether sensor crystals (PC-quartz crystal) coated with fibrinogen could provide a platelet activating surface and induce platelet aggregation; and secondly, whether using this system, the flow rate and shear stress could influence platelet microaggregation.

Polystyrene-coated quartz crystals were coated with fibrinogen, a plasma protein, which is both necessary and sufficient for platelet interactions leading to adhesion and aggregation. In fact, an early feature of platelet activation by different agonists is exposure of specific glycoprotein receptors, particularly GPIIb/IIIa, to which fibrinogen binds with high affinity [25]. In fact, patients suffering from fibrinogen disorders have long bleeding times [26]. In addition, fibrinogen is adsorbed on biomaterial surfaces in much higher quantity than other adhesion proteins and it is known to be well adsorbed on polystyrene [27]. Perfusion of fibrinogen-coated sensors with PRP led, as monitored in

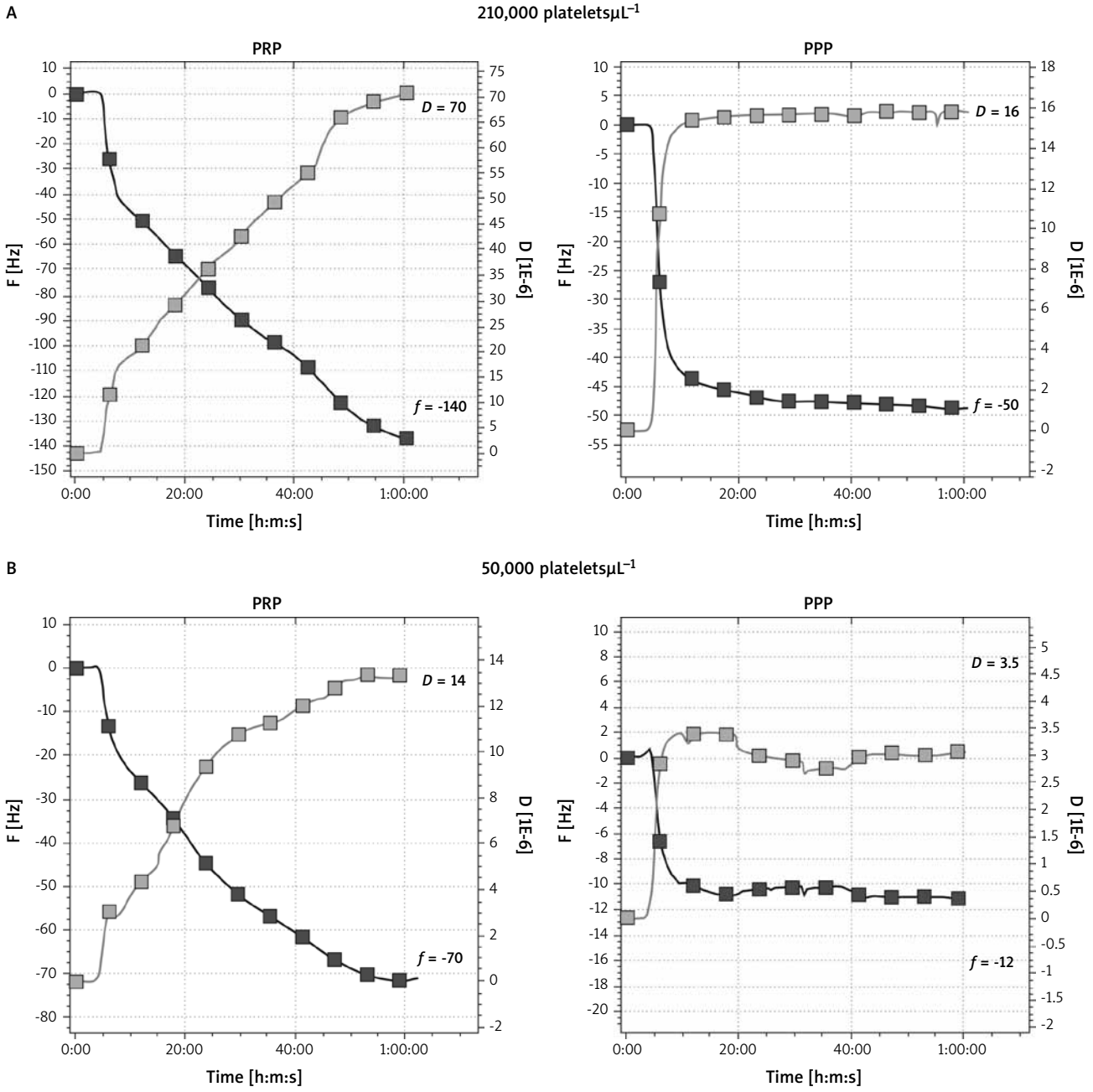

Fig. 6A–B. Effects of low platelet concentrations and platelet-poor plasma on frequency *f* and energy dissipation *D*. Perfusion of fibrinogen-coated PC-quartz crystals with low platelet concentrations leads to platelet aggregation. A. Representative tracings from the 3rd overtone recorded by the device show the effects of platelet-poor plasma (PPP) and 210,000 platelets/μL on *f* (blue line) and *D* (red line). B. Representative tracings from the 3rd overtone recorded by the device show the effects of platelet-poor plasma (PPP) and 50,000 platelets/μL on *f* (dark squares) and *D* (light squares)

real time by the device, to reduced *f* and increased *D*, and therefore accumulation of mass on the sensor surface in a platelet concentration-dependent manner confirmed by phase-contrast microscopy.

However, perfusion of fibrinogen-uncoated crystals with PRP led to reduced aggregation, supporting the hypothesis that fibrinogen plays an important role facilitating platelet adhesion and aggregation on the surface of sensor crystals. When confocal microscopy was performed on fibrinogen-coated PC-quartz crystals after perfusion of PRP, platelet cytoskeleton reorganization (visualized by anti-actin antibody) and the presence of activated GPIIb/IIIa receptors (stained with PAC-1 antibody) on the platelet membrane surface were shown. Furthermore, nanometre scale imaging analysis by AFM showed fried-egg-like platelets with budding granules and extended pseudopodia, that clearly indicated platelet activation [28]. Our results are consistent with previous studies which have shown that adhesion of platelets to materials coated with fibrinogen can lead to platelet activation [29, 30]. It is not surprising that fibrinogen-

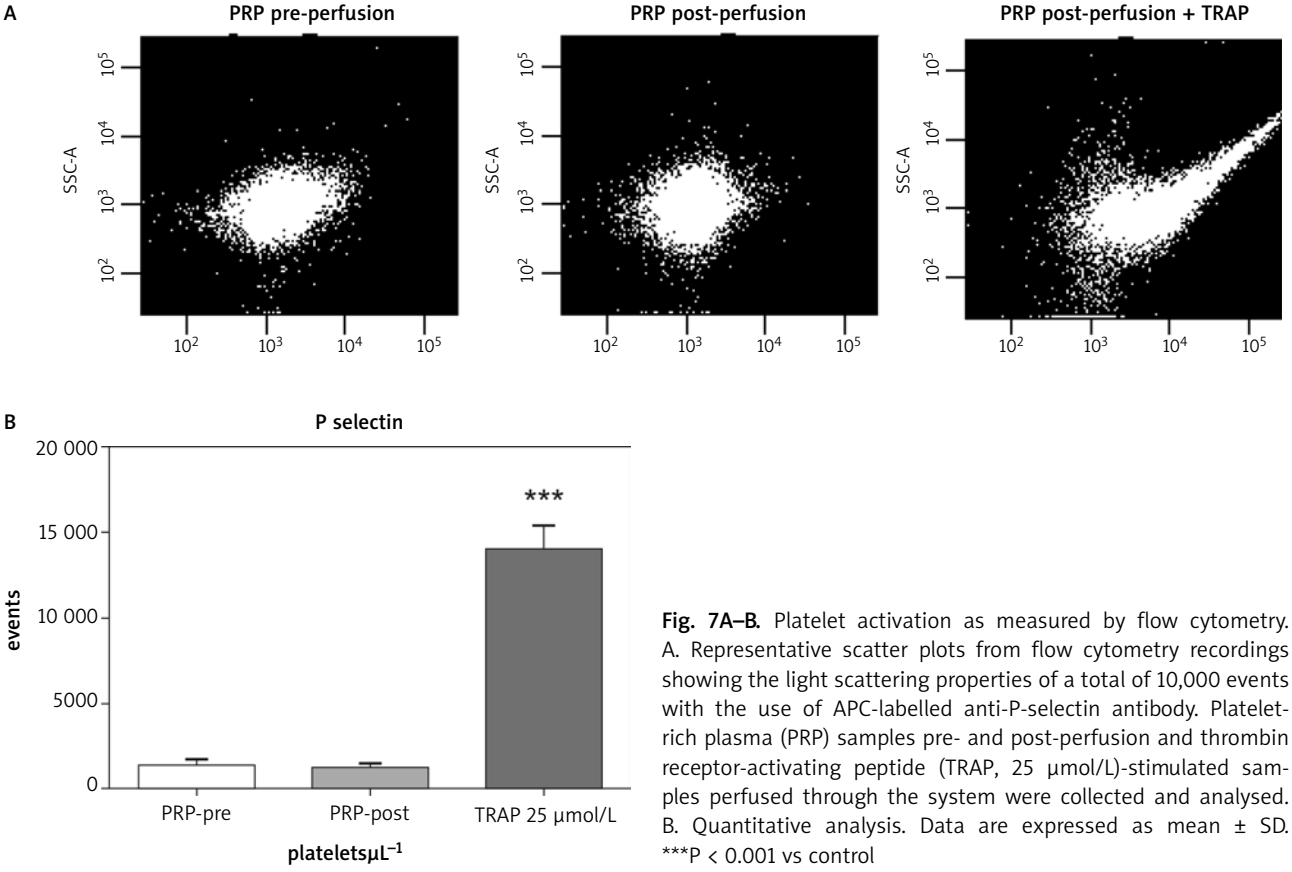

Fig. 7A–B. Platelet activation as measured by flow cytometry. A. Representative scatter plots from flow cytometry recordings showing the light scattering properties of a total of 10,000 events with the use of APC-labelled anti-P-selectin antibody. Platelet-rich plasma (PRP) samples pre- and post-perfusion and thrombin receptor-activating peptide (TRAP, 25 µmol/L)-stimulated samples perfused through the system were collected and analysed. B. Quantitative analysis. Data are expressed as mean ± SD. ***P < 0.001 vs control

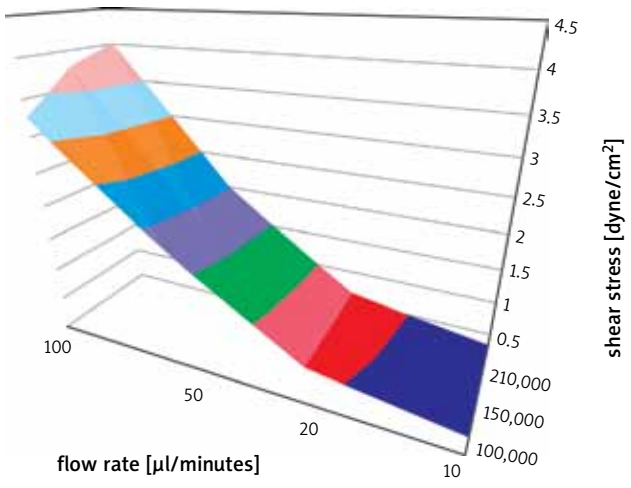

Fig. 8. Effects of flow rate and platelet number on shear stress. Platelet 3D shear stress profiles against flow rate (10, 20, 50 and 100 µL/minute) for increasing concentrations of platelets: 100,000; 150,000 and 210,000 platelets/µL at 37°C. The 3D map highlights the sharp increase in the shear stress associated with the flow rate between 20 to 50 µL/minute and 50 to 100 µL/minute for all three PRP concentrations.

Tab. I. Shear stress. Shear stresses calculated at 37°C for different concentrations of platelets at four flow rates (data are expressed as mean ± SD)

	100,000 platelets µL^{-1}	150,000 platelets µL^{-1}	210,000 platelets µL^{-1}
10 µL minute^{-1}	0.288 ±0.030	0.308 ±0.026	0.318 ±0.030
20 µL minute^{-1}	0.575 ±0.061	0.615 ±0.052	0.636 ±0.060
50 µL minute^{-1}	1.758 ±0.153	1.880 ±0.132	1.945 ±0.151
100 µL minute^{-1}	3.261 ±0.306	3.795 ±0.264	4.032 ±0.301

Shear stresses calculated at 37°C for different concentrations of platelets at four flow rates (data are expressed as mean ± s.d).

Tab. II. Thickness of the layer deposited on fibrinogen-coated crystals. Estimated thickness by Q-Tools and atomic force microscopy (AFM) of the layer deposited on the crystal surface after perfusion of different concentrations of platelet-rich plasma (PRP) for 30 minutes

PRP concentrations	Q-Tools (Voigt-based model)	AFM (Nova software)
100,000 platelets µL^{-1}	1.298 µm	570 nm
150,000 platelets µL^{-1}	72.165 nm	503.2 nm
210,000 platelets µL^{-1}	178.4 nm	1.314 µm

Estimated thickness by Q-Tools and Atomic Force Microscopy (AFM) of the layer deposited on the crystal surface after perfusion of different concentrations of platelet-rich plasma (PRP) for 30 minutes.

uncoated PC-crystals induced platelet aggregation. It is well known that platelet aggregation takes place when blood is exposed to foreign surfaces, and this phenomenon underpins the thromboembolic complications associated with the use of different prosthetic devices [31]. Interestingly, sensor-induced platelet activation and microaggregate formation are detected even for very low concentrations of platelets and limited to the platelet population in direct contact with the sensor surface. Other platelets flowing through a 40 µL flow chamber are not activated, as shown by the flow cytometry analysis of platelet P-selectin.

The use of a nanoscale resolution device enabled us to study and quantify the onset of platelet microaggregation and subsequent phenomena under conditions of low shear stress (< 4 dyne cm^{-2}).

Under situations of low shear stress, bound fibrinogen promotes platelets to adhere firmly via platelet GPIIb/IIIa receptors [32]. In fact, when fibrinogen-coated sensors were perfused with PRP, platelet microaggregation was demonstrated by phase-contrast microscopy and AFM and increased expression of activated GPIIb/IIIa receptors was shown by immunofluorescence microscopy. Previous studies adopted well-established and well-characterised models to carry out *ex vivo* measurements [15, 33]. These are based on large volume (mL min^{-1}), high shear rate (> 1000 s^{-1}) and high shear stress (> 100 dyne cm^{-2}) models. With recent advances in nanotechnology it is now possible to custom-design microfluidics systems which can perform high-throughput screening of multiple antiplatelet agents with low shear stresses requiring only a few microlitres of blood [34].

Nanotechnology, therefore, offers a unique scalability in the model validation of shear-dependant platelet microaggregation. The instrument used in our study is a commercially available research device equipped with only four flow chambers, making it less suitable for high-throughput screening.

However, this device allows real-time, *ex vivo*, high-sensitivity and precise measurements of platelet microaggregation that can be easily supplemented by direct imaging of platelet aggregates on the sensor crystals using standard phase-contrast microscopy, highly advanced confocal imaging, AFM or scanning electron microscopy (SEM). In a previous study QCM-D was used to follow platelet morphological changes by SEM focusing on the platelet primary adhesion process on a mix of fibronectin and albumin deposited on silica crystals [35]. Weber et al. [36] have investigated the binding kinetics of GPIIb/IIIa to polymer-adsorbed fibrinogen using QCM-D, correlating the results with platelet adhesion to the polymer surfaces by SEM. However, the work presented here is part of a PhD thesis performed in our lab where the QCM-D was used for the first time to characterize platelet microaggregation under flow conditions with nanoscale resolution [37]. In fact, the presence of platelet microaggregates deposited on the sensor surface was detected in real time by the device and demonstrated by direct imaging of the sensor crystals by AFM.

The linear Sauerbrey equation has been widely used to quantify the mass as an increase in the mass bound to the sensor causes the crystal's oscillation f to decrease. However, the Sauerbrey equation does not apply in situations where the mass bound to the sensor surface behaves as a complex viscoelastic layer. Previous studies on cell adhesion using QCM have demonstrated that cells attached to the sensor surface produce significant variability in f shifts and do not behave as elastic masses. In fact, in cellular adsorption applications, the f and Sauerbrey relationship underestimate the adsorbed mass of cells and the D parameter becomes essential to fully characterize the adsorption of a viscoelastic cellular structure [20, 21]. Interestingly, the inapplicability of the Sauerbrey equation has been demonstrated in a study with platelets where the f response produced by binding human platelets to collagen was compared to the calculated mass bound using ^{51}Cr radiolabelling of platelets. The mass value estimated by the Sauerbrey equation was found to be 200 times less than the actual bound mass based on the radiolabelled measurements [38]. If the adsorbed layer is homogeneous across the crystal, it is also theoretically possible to estimate the mass using a Voigt-based viscoelastic model included in the Q-Tools software combining and fitting both f and D [39]. However, in our experiments the distribution of the platelet aggregates (not always uniform through the sensor surface, as shown by phase-contrast and AFM), and the complexity in the viscoelastic structure of the platelet aggregate layer, make the software unsuitable for the measurement of mass. Therefore f and D values are used to quantify the changes in platelet aggregation.

The sensitivity limits of the system allow for platelet measurement within the sensor area which is almost 1000 times larger than a platelet. Although the adhesion of platelets to the substrate was expected to increase the shear stress as the channel size becomes reduced, an aggregate had an average height measured by AFM that accounted for only 0.5% reduction of the total chamber depth, facilitating on the other hand the instrument's precise measurements. In addition, the detection of platelet activation measured by flow cytometry only after perfusion of PRP in the presence of agonist demonstrates that this method mimics the platelet behaviour at microvasculature level where platelets become activated just in the place of injury. Real-time measurements at very low concentrations of platelets (50,000 μL^{-1}) also point to the ability of this device to quantify platelet function in low platelet concentration samples such as from patients with thrombocytopenia.

In conclusion, we have shown that platelet microaggregates are formed on fibrinogen-coated surfaces under low shear stress and this deposition can be quantified with great sensitivity by QCM-D. Thus, platelet microaggregate biology and physiology can be effectively studied using nanoscale resolution devices.

Acknowledgments

We are grateful to Paul Jurasz, John Booth, Alan Gaffney and Carsten Ehrhardt for helpful discussions and to Esther

Rufino for technical help. The work was supported by a Science Foundation Ireland (SFI) PI grant to MWR and an SFI-RFP grant to CM. CM is an SFI Stokes Lecturer.

References

1. Ginsberg MH, Loftus J, Plow EF. Platelets and the adhesion receptor superfamily. Prog Clin Biol Res 1988; 283: 171-195.
2. Ginsberg MH, Xiaoping D, O'Toole TE, Loftus JC, Plow EF. Platelet integrins. Thromb Haemost 1993; 70: 87-93.
3. Needleman P, Moncada S, Bunting S, Vane JR, Hamberg M, Samuelsson B. Identification of an enzyme in platelet microsomes which generates thromboxane A2 from prostaglandin endoperoxides. Nature 1976; 261: 558-560.
4. Born GV. Effects of adenosine diphosphate (ADP) and related substances on the adhesiveness of platelets in vitro and in vivo. Br J Haematol 1966; 12: 37-38.
5. Sawicki G, Salas E, Murat J, Miszta-Lane H, Radomski MW. Release of gelatinase A during platelet activation mediates aggregation. Nature 1997; 386: 616-619.
6. Cramer EM, Savidge GF, Vainchenker W, Berndt MC, Pidard D, Caen JP, Masse JM, Breton-Gorius J. Alpha-granule pool of glycoprotein IIb-IIIa in normal and pathologic platelets and megakaryocytes. Blood 1990; 75: 1220-1227.
7. O'Brien JR. The adhesiveness of native platelets and its prevention. J Clin Pathol 1961; 14: 140-9.
8. Born GV. Aggregation of blood platelets by adenosine diphosphate and its reversal. Nature 1962; 194: 972-979.
9. Cardinal DC, Flower RJ. The electronic aggregometer: a novel device for assessing platelet behavior in blood. J Pharmacol Method 1980; 3: 135-158.
10. Frojmovic MM. From in vitro blood rheology to useful bedside instrumentation for cardiovascular diseases: history and challenges. Ann Biomed Eng 2008; 36: 528-533.
11. Sakariassen KS, Turitto VT, Baumgartner HR. Recollections of the development of flow devices for studying mechanisms of hemostasis and thrombosis in flowing whole blood. J Thromb Haemost 2004; 2: 1681-1690.
12. Podda GM, Bucciarelli P, Lussana F, Lecchi A, Cattaneo M. Usefulness of PFA-100 testing in the diagnostic screening of patients with suspected abnormalities of hemostasis: comparison with the bleeding time. J Thromb Haemost 2007; 5: 2393-2398.
13. Hayward CP, Harrison P, Cattaneo M, Ortel TL, Rao AK, Platelet Physiology Subcomittee of the scientific and Standardization Committee of the International Society of Thrombosis and Haemostasis. Platelet function analyzer (PFA)-100 closure time in the evaluation of platelet disorders and platelet function. J ThrombHaemost 2006; 4: 312-319.
14. Sakariassen KS, Hanson SR, Cadroy Y. Methods and Models to Evaluate Shear-Dependent and Surface Reactivity-Dependent Antithrombotic Efficacy. Thromb Res 2001; 104: 149-174.
15. Zwaginga JJ, Sakariassen KS, Nash G, King MR, Heemskerk JW, Frojmovic M, Hoylaerts MF. Flow-based assays for global assessment of hemostasis. Part 2: current methods and considerations for the future. J ThrombHaemost 2006; 4: 2716-2717.
16. Sauerbrey G. Verwendung von Schwingquarzen zur wägung dünner schichten und zur mikrowägung. Z Phys 1959; 155: 206-222.
17. Matsuda T, Kishida A, Ebato H, Okahata Y. Novel instrumentation monitoring in situ platelet adhesivity with a quartz crystal microbalance. ASAIO Journal 1992; 38: M171-M173.
18. Kawakami K, Harada Y, Sakasita M, Nagai H, Handa M, Ikeda Y. A new method for continuous measurement of platelet adhesion under flow conditions. ASAIO Journal 1993; 39: M558-M560.
19. Hook F, Rodahl M, Brzezinski P, Kasemo B. Energy dissipation kinetics for protein and antibody-antigen adsorption under shear oscillation on a quartz crystal microbalance. Langmuir 1998; 14: 729-734.
20. Fredriksson C, Kihlman S, Rodahl M, Kasemo B. The piezoelectric quartz crystal mass and dissipation sensor: A means of studying cell adhesion. Langmuir 1998; 14: 248-251.
21. Marx KA. Quartz crystal microbalance: A useful tool for studying thin polymer films and complex biomolecular systems at the solution-surface interface. Biomacromolecules 2003; 4: 1099-1120.
22. Dixon M. Quartz crystal microbalance with dissipation monitoring: Enabling real-time characterization of biological materials and their interactions. J Biomol Tech 2008; 19: 151-158.
23. Radomski M, Moncada S. An improved method for washing of human platelets with prostacyclin. Thromb Res 1983; 30: 383-389.
24. Li X, Radomski A, Corrigan OI, Tajber L, De Sousa Menezes F, Endter S, Medina C, Radomski MW. Platelet compatibility of PLGA, chitosan and PLGA-chitosan nanoparticles. Nanomedicine (Lond) 2009; 4: 735-746.
25. Tailor A, Cooper D, Granger DN. Platelet-vessel wall interactions in the microcirculation. Microcirculation 2005; 12: 275-285.
26. 26 Vu D, Neerman-Arbez M. Molecular mechanisms accounting for fibrinogen deficiency: from large deletions to intracellular retention of misfolded proteins. J Thromb Haemost 2007; 5: 125-131.
27. Chinn JA, Horbett TA, Ratner BB. Baboon fibrinogen adsorption and platelet adhesion to polymeric materials. Thromb Haemost 1991; 65: 608-617.
28. Karagkiozaki V, Logothetidis S, Kalfagiannis N, Lousinian S, Giannoglou G. Atomic force microscopy probing platelet activation behavior on titanium nitride nanocoatings for biomedical applications. Nanomedicine 2009; 5: 64-72.
29. Tsai WB, Grunkemeier JM, Horbett TA. Human plasma fibrinogen adsorption and platelet adhesion to polystyrene. JBiomed Mater Res 1999; 44: 130-139.
30. Zhang M, Wu Y, Hauch K, Horbett TA. Fibrinogen and von Willebrand factor mediated platelet adhesion to polystyrene under flow conditions. J Biomater Sci Polym Ed 2008; 19: 1383-1410.
31. Salzman EW. Influence of antiplatelet drugs on platelet-surface interactions. Adv Exp Med Biol 1978; 102: 265-283.
32. Savage B, Saldívar E, Ruggeri ZM. Initiation of platelet adhesion by arrest onto fibrinogen or translocation on von Willebrand factor. Cell 1996; 84: 289-297.
33. Kroll MH, Hellums JD, McIntire LV, Schafer AI, Moake JL. Platelets and shear stress. Blood 1996; 88: 1525-1541.
34. Gutierrez E, Petrich BG, Shattil SJ, Ginsberg MH, Groisman A, Kasirer-Friede A. Microfluidic devices for studies of shear-dependent platelet adhesion. Lab Chip 2008; 8: 1486-1495.
35. Fatisson J, Merhi Y, Tabrizian M. Quantifying blood platelet morphological changes by dissipation factor monitoring in multilayer shells. Langmuir 2008; 24: 3294-3299.
36. Weber N, Wendel HP, Kohn J. Formation of viscoelastic protein layers on polymeric surfaces relevant to platelet adhesion. J Biomedl Mater Res A 2005; 72A: 420-427.
37. Santos-Martinez MJ. A novel method for the measurement of flow-induced platelet activation at nanoscale resolution level. Thesis (PhD).Trinity College Dublin, 2009.
38. Muratsugu M, Romaschin AD, Thompson M. Adhesion of human platelets to collagen detected by 51Cr labelling and acoustic wave sensor. Anal Chim Acta 1997; 342: 23-29.
39. Voinova MV, Rodahl M, Jonson M, Kasemo B. Viscoelastic acoustic response of layered polymer films at fluid-solid interfaces: continuum mechanics approach. Phys Scr 1999; 59: 391-396.